

Cryogenic Fourier transform spectrometer for infrared spectral calibrations from 4 to 20 micrometers

Solomon I. Woods, Simon G. Kaplan, Timothy M. Jung, Adriaan C. Carter, and Raju U. Datla
National Institute of Standards and Technology, Gaithersburg, MD 20899

ABSTRACT

We present initial performance data from a cryogenic Fourier transform spectrometer (Cryo-FTS) designed for low-background spectral infrared calibrations. The Cryo-FTS operates at a temperature of approximately 15 K and has been integrated into an infrared transfer radiometer containing a calibrated Si:As blocked impurity band (BIB) detector. Because of its low operating temperature, the spectrometer exhibits negligible thermal background signal and low drift. Data from tests of basic spectrometer function, such as modulation efficiency, scan jitter, spectral range, spectral resolution and sweep speed will be presented. We will also discuss calibration techniques and results pertinent to operation of the Cryo-FTS as part of a calibration instrument, including background, signal offset and gain, and spectral noise equivalent power. The spectrometer is presently limited to wavelengths below 25 micrometers but can be in principle extended to longer wavelengths by replacing its KBr beamsplitter with another beamsplitter engineered for use beyond 25 micrometers.

Keywords: infrared, radiometry, calibration, cryogenic, Fourier-transform spectrometer

1. INTRODUCTION

Since 2001, the Low-Background Infrared (LBIR) facility at the National Institute of Standards and Technology (NIST) has provided onsite radiometric calibration of the collimated output beam irradiance from infrared (IR) ground test chambers used in the development and testing of missile defense sensors. These calibrations have been performed using the Ballistic Missile Defense Transfer Radiometer (BXR), a portable, cryogenic radiometer with a 7 cm entrance pupil [1]. The BXR is calibrated against an absolute cryogenic radiometer (ACR) at NIST and uses a Si:As blocked-impurity band (BIB) detector and a set of 10 bandpass filters from 2 μm to 14 μm wavelength to provide coarse spectral coverage over the wavelength range of interest to the missile-defense community. The uncertainty ($k=1$) in these calibrations is typically $\pm 3\%$ over a range of approximately 10^{-14} W/cm² to 10^{-9} W/cm².

While the BXR has been very successful in helping to confirm the radiometric accuracy and year-to-year stability of various ground test chambers, there has been considerable interest in the community in finer and more continuous spectral characterization of the chamber output beams. A chamber that consists of a blackbody source (which can be calibrated at LBIR for radiance temperature), a set of apertures, and metallic collimating and steering mirrors should have a simple spectral response that can be accurately modeled with the Planck equation, measured mirror reflectances, and diffraction analysis. However, there is considerable interest in more spectrally complex or tunable sources, which cannot be adequately characterized or calibrated with a discrete filter radiometer such as the BXR. NIST has thus developed a new portable cryogenic radiometer, the Missile Defense Transfer Radiometer (MDXR), which includes several enhancements relative to BXR, and specifically a cryogenic Fourier-transform spectrometer (Cryo-FTS) designed to provide continuous spectral coverage from 4 μm to 20 μm with < 1 cm⁻¹ resolution.

The Cryo-FTS was constructed to NIST specifications under contract to Telops, Inc. Its design, construction, and preliminary ambient temperature performance have been reported previously [2]. In this paper, we describe the results of performance specification tests at cryogenic (15 K) conditions, and initial results of radiometric accuracy tests performed with the Cryo-FTS mounted in the MDXR.

2. DESIGN OF THE CRYO-FTS

The Cryo-FTS optical layout is shown in Figure 1 below [3]. All of the mechanical and IR optical components, including the BIB detector and preamplifier, are contained in the vacuum cryogenic space of the MDXR chamber. The metrology laser beam from a single-mode 783 nm diode laser is fed into the vacuum chamber using a single-mode optical fiber. The collimated metrology beam is passed through the Michelson interferometer, parallel to the IR beam, and is collected by an array of multimode fibers designed to measure the optical path difference in the interferometer as

well as wavefront tilt. The laser light is fed back out of the vacuum space to photodiode detectors in the ambient control electronics box. The beamsplitter and compensator are made from KBr substrates, with a coating on the beamsplitter to optimize modulation efficiency from 4 μm to 20 μm wavelength. The moving mirror mechanism is a porch-swing design with steel flexures that provides a maximum optical path difference of 1.4 cm. Wavefront alignment is maintained using a two-axis voice-coil actuator on a fold mirror placed on the moving mirror side of the beamsplitter. The IR beam, metrology beam, and white light beam for determination of zero optical path difference (ZPD) are displaced horizontally across the beamsplitter. Provision is made in the control software for an offset in the optimum wavefront alignment mirror tilt between the metrology and infrared beams.

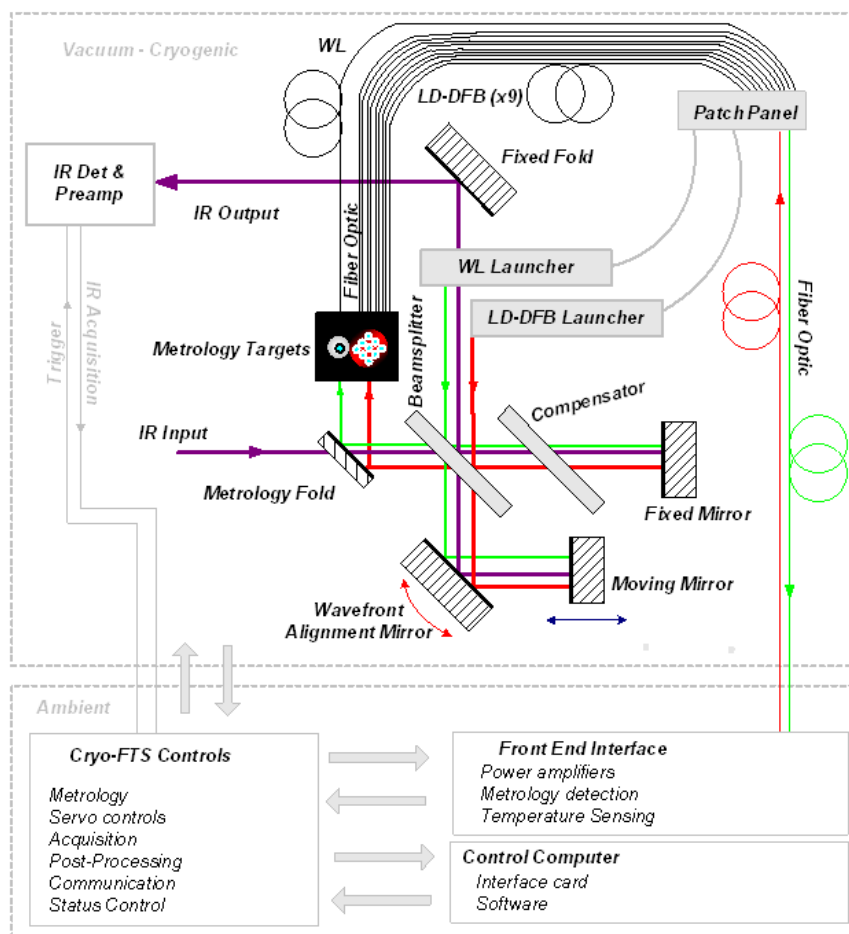


Figure 1. Optical block diagram of the Cryo-FTS, showing the optical components and a schematic of the signal handling scheme.

The Cryo-FTS clear aperture for the collimated input IR beam is 2.0 cm. Figure 2 shows a photograph of the Cryo-FTS as mounted in the MDXR. The MDXR accepts a highly collimated 7.0 cm diameter input beam, which is converted to a 2.0 cm beam with 3.5x increased divergence. After passing through the Cryo-FTS, the output beam travels through a set of filter wheels which contain spectral bandpass and neutral density filters, as well as two orthogonal fixed polarizers and a rotatable polarizer, before being focused onto a Si:As BIB detector using an off-axis paraboloidal mirror. The detector is temperature stabilized at 10 K and mounted on a motorized xyz stage for alignment.

The MDXR also contains an onboard blackbody source with a 0.5 mm diameter aperture and 7 cm diameter collimating telescope (on the opposite side of the optics plate shown in Figure 2) which can be rotated into place in front of the defining aperture to allow the Cryo-FTS to alternately view the external beam or a stable internal reference source which can be calibrated with an absolute cryogenic radiometer (ACR).

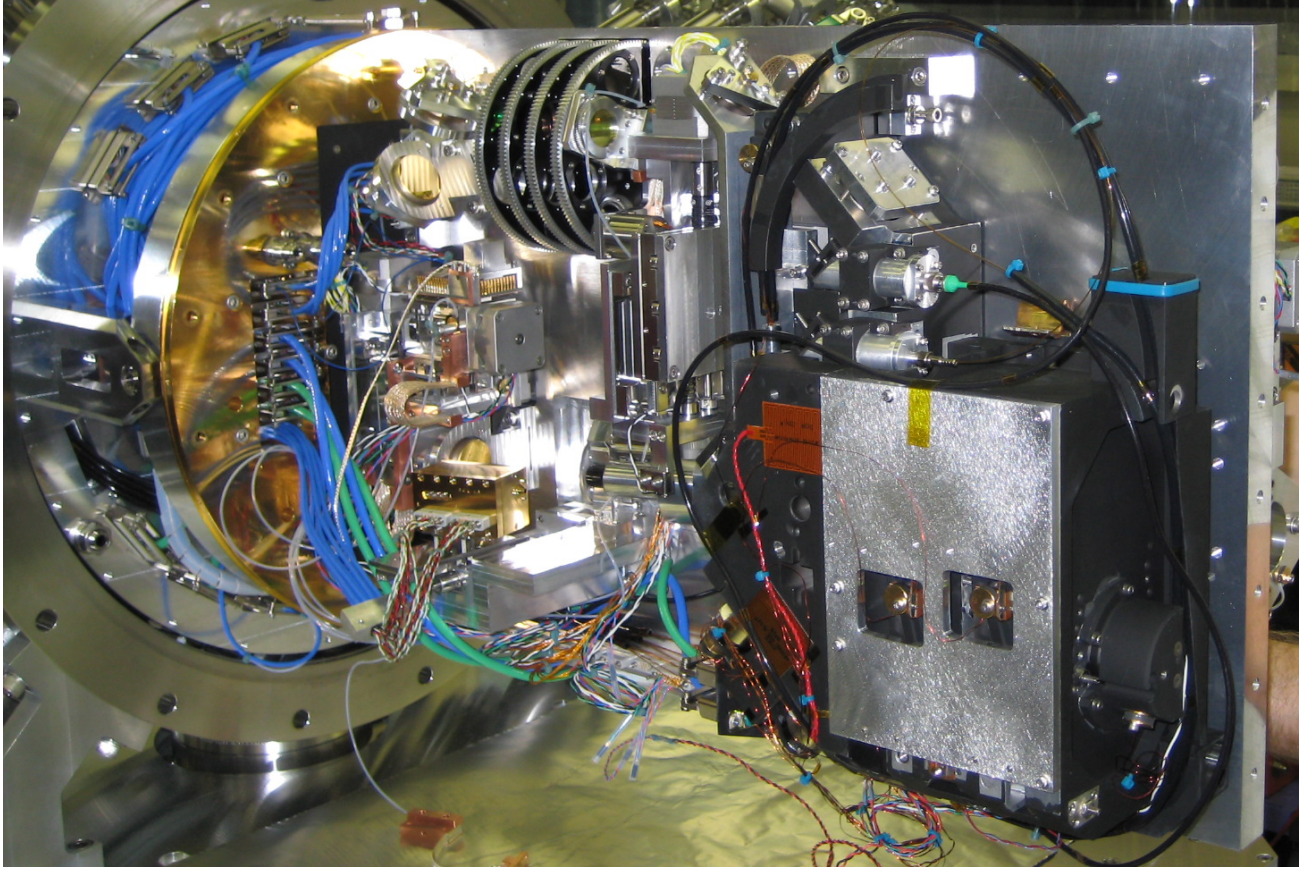


Figure 2. The Cryo-FTS (lower right) as mounted in the MDXR chamber. The output beam from the Cryo-FTS passes through the filter wheel assembly in the top center of the picture before striking a fold mirror and being focused down to the detector stage by the off-axis paraboloidal mirror in the upper left.

3. OPTICAL PERFORMANCE OF THE CRYO-FTS

The Cryo-FTS was initially tested under vacuum cryogenic conditions mounted in a test chamber similar to the MDXR chamber. The temperature of the instrument was approximately 15 K and the pressure in the chamber was less than 10^{-6} mbar. A 1.7 cm defining aperture was used for these tests, and the Cryo-FTS viewed external sources through a ZnSe vacuum window. Tests were performed to determine the modulation efficiency, spectral resolution, and scan-to-scan repeatability of the spectrometer. The modulation efficiency was tested using a 3.39 μm HeNe laser. We define modulation efficiency ε as the ratio of modulated output flux at the detector to the (constant) input flux at the entrance pupil of the Cryo-FTS. For a monochromatic source, the output intensity I at the detector plane as a function of optical path difference x is given by

$$I = \frac{I_0}{2} (1 + 2\varepsilon \cos(2\pi\nu x)) \quad (1)$$

where I_0 is the input flux, and ν is the wavenumber of the source [4]. Since the detector output from the Cryo-FTS processing electronics is ac-coupled, a separate measurement of the dc voltage level of the detector is performed, and the ε is calculated as

$$\varepsilon = \frac{1}{4} \left(\frac{AC_1 - AC_2}{DC_1 - DC_2} \right) \quad (2)$$

where subscripts 1 and 2 respectively refer to measurements made with the laser signal present, or blocked. The blocked measurements are made to eliminate ambient temperature background flux that makes it into the Cryo-FTS entrance pupil through the vacuum window. In this definition, the maximum possible value of ε for a perfect Michelson interferometer is 0.5. Figure 3 shows an example of a modulation efficiency measurement taken over the full scan range of the instrument (0.85 cm^{-1} resolution) at 0.5 cm/s optical path difference scan rate [5].

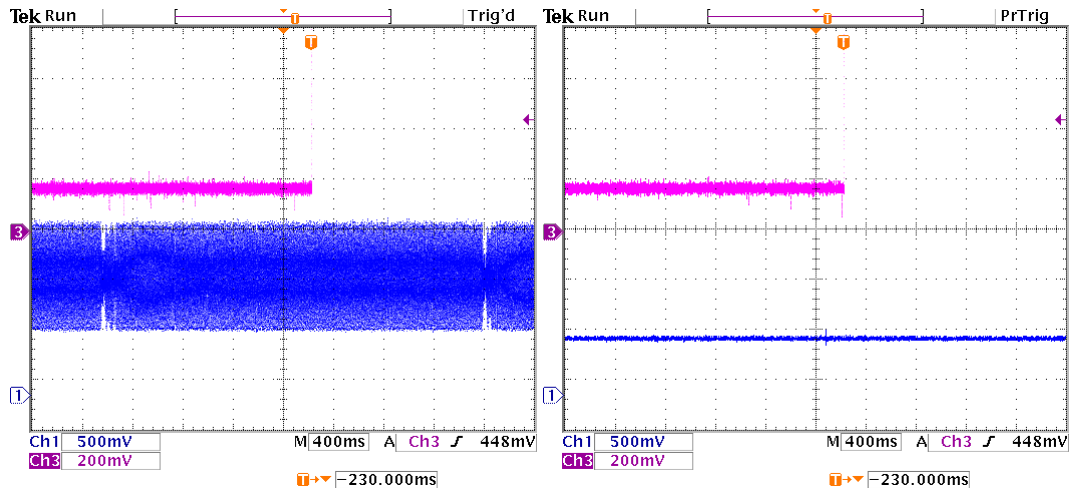


Figure 3. DC-coupled oscilloscope traces for the Cryo-FTS detector output with a $3.39 \mu\text{m}$ laser input and conditions described in the text. The left panel is with the laser input and the right panel with the laser blocked. The amplitude of the modulated signal in the left frame is compared to the background level in the right frame to derive the modulation efficiency (Eq. 2).

In this case we measured $\varepsilon = 0.44$. The Cryo-FTS was found to have modulation efficiency between 0.39 and 0.45 for all tested resolutions between 0.85 cm^{-1} and 30 cm^{-1} and optical path difference scan rates between 0.3 cm/s and 2 cm/s , falling off to $\varepsilon = 0.23$ at a scan rate of 8 cm/s . For radiometric measurements with the MDXR, 1 cm/sec scan rate is found to be adequate. While we have not directly measured the modulation efficiency at longer wavelengths, it should be expected to be at least as large out to $20 \mu\text{m}$ given the measured reflectance and transmittance of the beamsplitter.

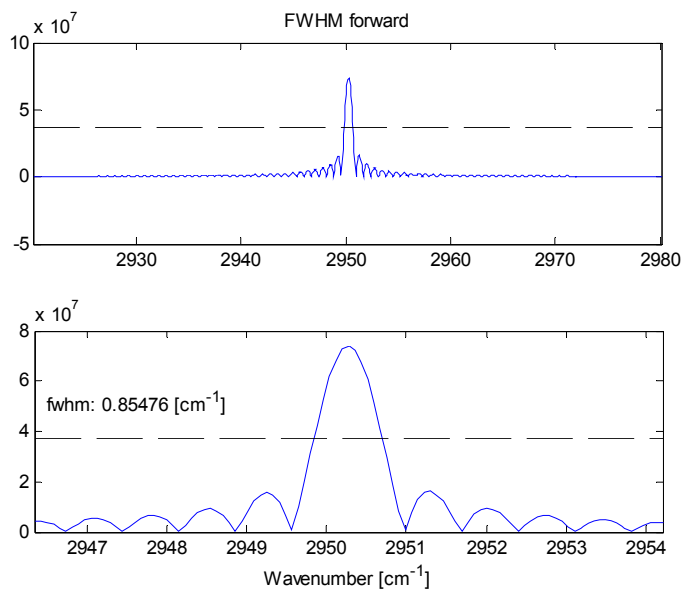


Figure 4. Spectrum of the $3.39 \mu\text{m}$ HeNe laser at the maximum spectral resolution of the Cryo-FTS, showing a FWHM of 0.85 cm^{-1} .

The next performance test, also using the 3.39 μm HeNe laser input, was a test of spectral resolution. Figure 4 shows the Fourier transform of several interferograms acquired at 1.41 cm optical path difference and 0.5 cm/s optical path difference scan rate [5]. The linewidth of the HeNe laser is nominally less than 300 MHz, so the spectrum should show the expected sinc function of the instrument response function, clearly seen in the bottom frame of Figure 4, which also shows the full width half-maximum (FWHM) of 0.85 cm^{-1} corresponding to the maximum spectral resolution of the Cryo-FTS.

Finally, the Cryo-FTS was used to view an external blackbody source at 400 K. The scan-to-scan repeatability of the phase-corrected spectra was examined over the spectral range from 2000 cm^{-1} to 2400 cm^{-1} for 30 scans in both the forward and reverse directions. The standard deviation in the spectra over this range were found to vary from 0.18 % at 16 cm^{-1} resolution to 0.97 % at 0.85 cm^{-1} resolution.

4. INITIAL RADIOMETRIC TESTING OF THE CRYO-FTS

The goal of the Cryo-FTS in MDXR is to be able to acquire calibrated irradiance spectra of user sources with a relative expanded radiometric uncertainty of 1 % . The short term stability of the scanning mechanism appears to be able to meet this requirement at moderate spectral resolutions. However, we must also investigate the stability of the system over the time required to make measurements of user sources and compare with a stable, calibrated reference source. In addition, we must consider the contribution of systematic uncertainty components such as nonlinearity, inter-reflections, stray light, and FTS phase error. Initial characterization was performed with the Cryo-FTS in its test chamber using a 1.5 cm defining aperture, mounted to the output of the LBIR 10 cm collimator, which produces a well-collimated output beam from a cryogenic blackbody source and filter wheel assembly. Figure 5 shows the stability of spectral scans of 1 min duration taken over a period of approximately 2 h at a resolution of 4 cm^{-1} , with a blackbody temperature of 600 K.

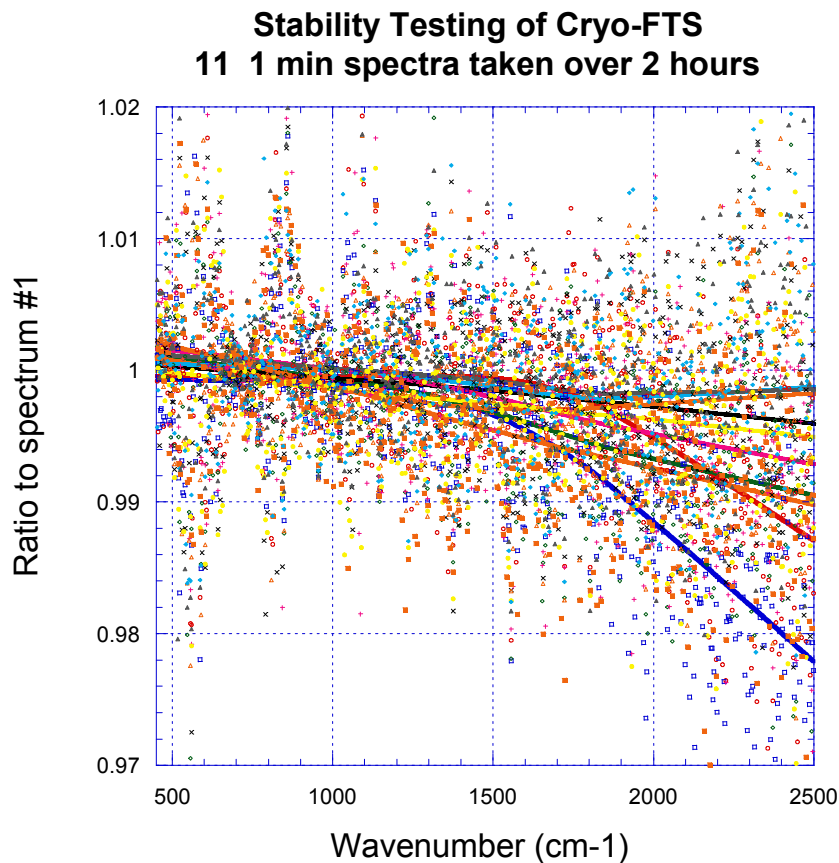


Figure 5. Ratio of 10 spectra over 2 h viewing output from 600 K blackbody source, to first spectrum.

There is amplifier noise with an amplitude of about 1.5 % in these spectra, but if we perform a locally-weighted least squares fit to smooth through the noise, it is apparent that the baseline is stable to within 1 % over this period except for one curve which falls outside the range above 2000 cm^{-1} . This indicates that the Cryo-FTS should have adequate stability at least over the typical time of several hours for changing and stabilizing cryogenic blackbody source temperatures over ranges of hundreds of kelvin.

A test for linearity of response and background or stray light rejection was performed by changing the blackbody aperture through 6 different sizes and performing measurements with the Cryo-FTS from 1 min (apertures 1 to 4) through 5 min (apertures 5 and 6). The spectra and spectrally integrated incident power levels (as calibrated with an ACR) are shown in Figure 6.

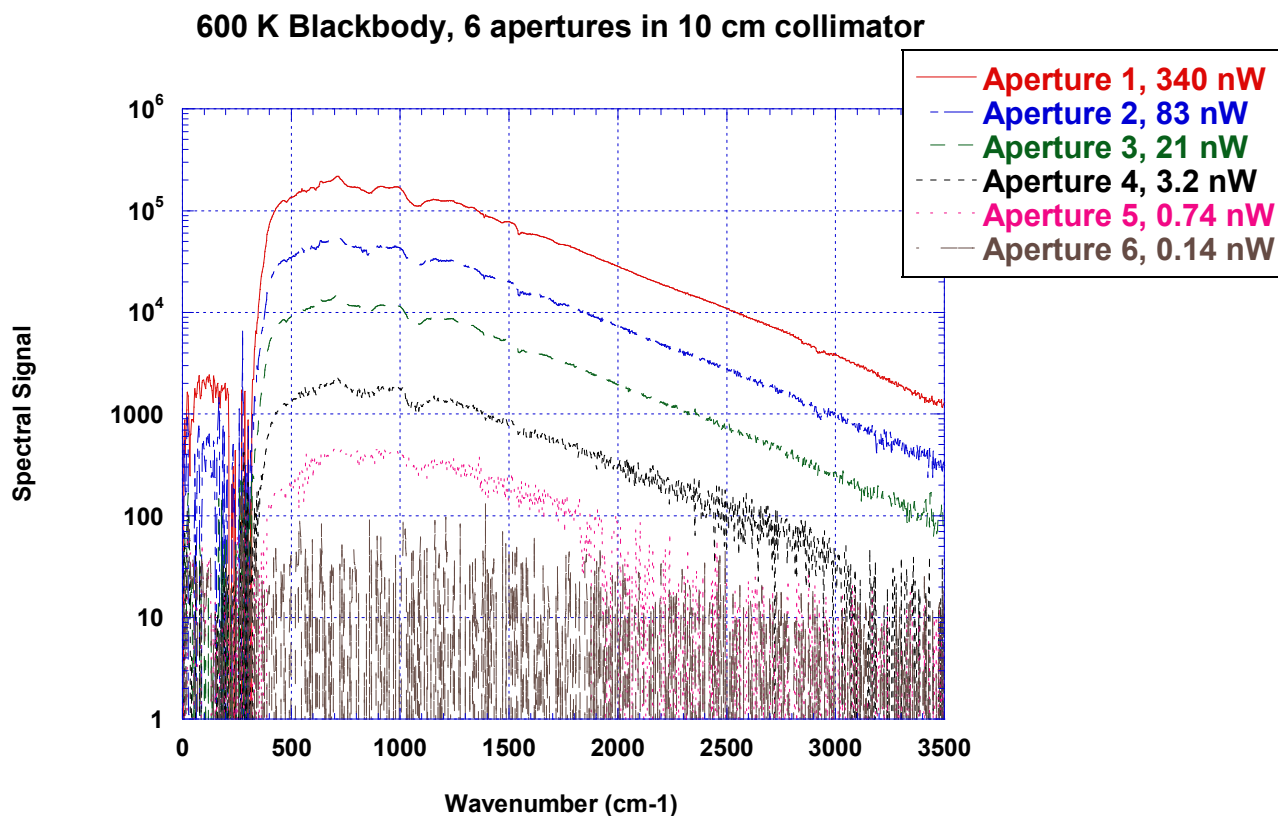


Figure 6. Cryo-FTS spectra for 600 K blackbody temperature and set of 6 apertures, with spectrally integrated incident power levels (measured with ACR) indicated.

Several features are apparent in these spectra. First of all, the two highest power levels, apertures 1 and 2, show effects of detector nonlinearity as false signal below the 350 cm^{-1} cutoff of the KBr beamsplitter. The lowest signal level, aperture 6, is below the noise level for 5 min averaging and 4 cm^{-1} resolution. We have also made measurements with the cold shutter closed and confirmed that any modulated signal coming from stray light or background thermal radiation is less than $\approx 3 \times 10^{-4}$ of the signal from the largest aperture with 600 K radiation, as would be expected in the 15 K chamber environment. Ratios of the spectrally integrated power levels measured with successively smaller pairs of apertures are shown in Table 1. The first two ratios are smaller than expected, consistent with saturation effects in the Si BIB detector, while the third ratio is within 1 % of the expected level. More systematic tests of the Cryo-FTS response are planned using the full aperture of the MDXR.

Ratio	Measured	Expected
Apt 1/Apt 2	3.87 ± 0.04	4.06
Apt 2/Apt 3	3.77 ± 0.04	4.00
Apt 3/Apt 4	6.56 ± 0.07	6.52

Table 1. Measured (along with standard uncertainties) and expected integrated spectral ratios for blackbody apertures 1 through 4.

Another test of response linearity can be seen in Figure 7, which shows the ratio of spectra with aperture 3 at blackbody temperatures of 600 K and 500 K compared to the calculated Planck ratios. After smoothing through the noise in the spectral traces, we see that the ratioed spectra show agreement within approximately 1.5 K with the calculated ratios. These spectra were obtained with about 5 hours between scans.

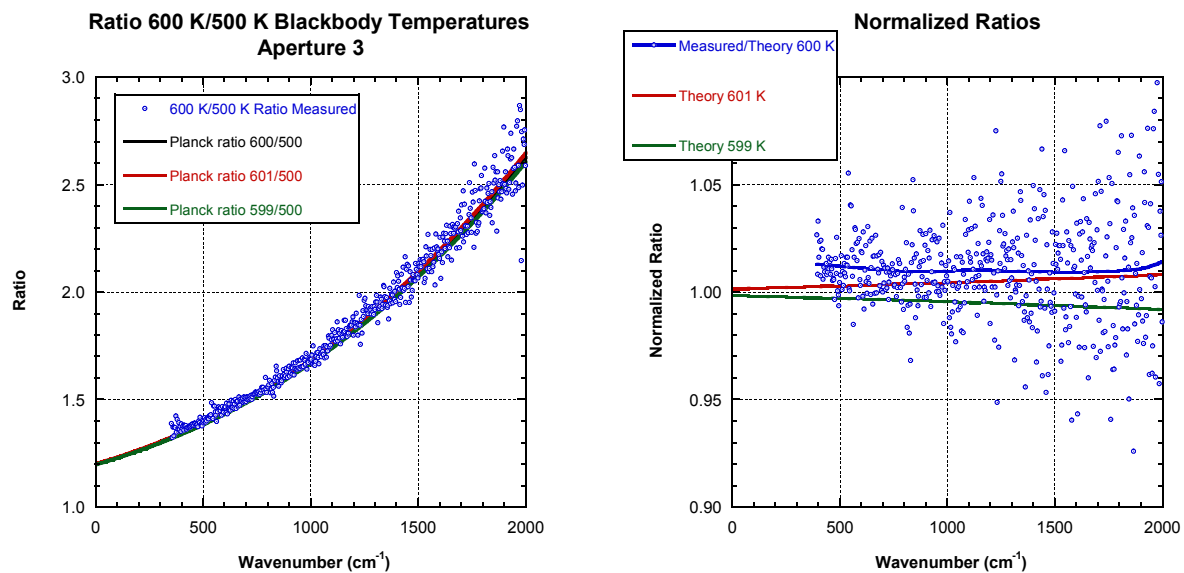


Figure 7. Measured ratios of spectra at 600 K and 500 K blackbody temperatures compared to ratios of corresponding Planck functions. The right frame shows measured spectral ratio divided by Planckian spectral ratio, along with curves showing the expected spectral deviations for ± 1 K error in radiance temperature.

5. RADIOMETRIC PERFORMANCE OF THE CRYO-FTS IN MDXR

The Cryo-FTS was mounted in the MDXR vacuum chamber, as shown in Figure 2, and optically aligned to within < 0.5 mrad using retroreflection from an optically flat reference surface adjacent to the IR beam entrance port of the spectrometer. The optical fiber feedthroughs were replaced with longer (15 m) pieces, and the As:Si BIB detector/amplifier package was replaced with one that has been found to have $\sim 10x$ reduced rf noise level. With the Cryo-FTS viewing input flux from the full 7 cm aperture of the radiometer, it is possible to begin to assess its expected response function and spectral noise floor when viewing user sources.

Figure 8 shows the Cryo-FTS spectral signal acquired with 35 s of averaging while viewing the internal MDXR blackbody source at a temperature of 300 K. The spectrally integrated flux collected by the As:Si BIB detector,

bypassing the Cryo-FTS, is 2.18 nW with a standard uncertainty of ± 0.05 nW. It is clear from the spectra shown in Figure 8(a) that the spectral response of the Cryo-FTS system falls off at low wavenumber because of absorption in the KBr beamsplitter, and at high wavenumber largely because of the Si:As BIB photon detector responsivity. From the repeatability data shown in frame (b), we can calculate the noise floor of the system at the peak response near 600 cm^{-1} as approximately 14 fW in a 4 cm^{-1} interval and 1 min of averaging. This would imply a minimum detectable irradiance at the MDXR defining aperture of $\sim 0.4\text{ fW/cm}^2$ in this spectral bin. More extensive tests over a range of blackbody temperatures and comparisons with the broadband flux measured by the ACR are under way.

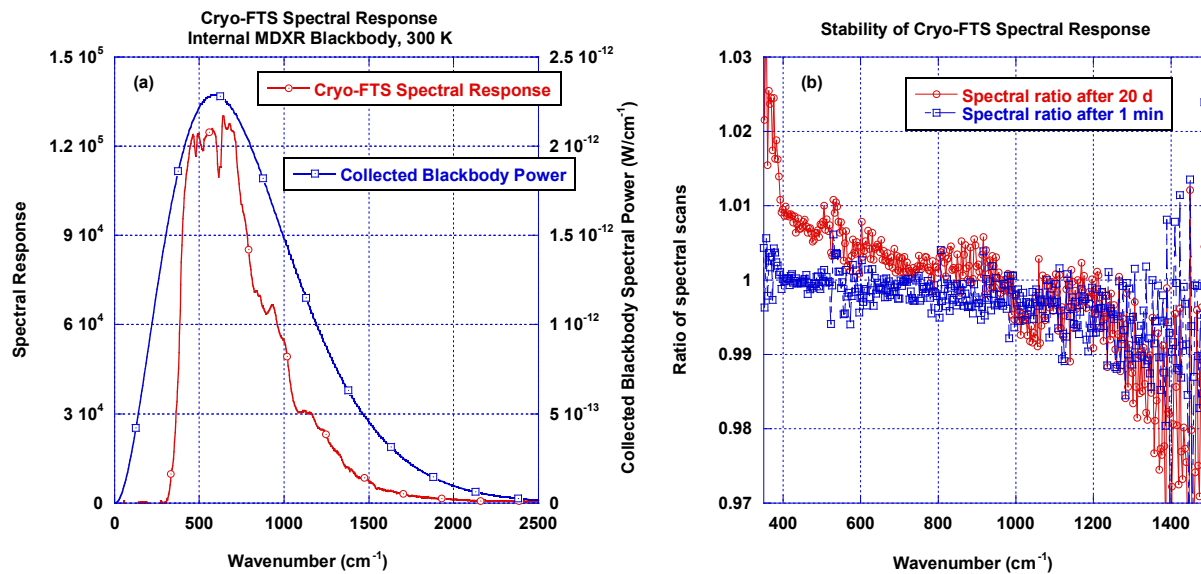


Figure 8. Spectral response of Cryo-FTS when viewing internal MDXR blackbody source at 300 K. Frame (a) compares the measured spectrum with the expected flux per wavenumber received from a Planckian source, while frame (b) shows the repeatability of the spectral response over short (1 min) and long (20 d) intervals.

6. CONCLUSIONS

The Cryo-FTS system appears to have the sensitivity to perform adequately for spectral radiometric characterization of irradiance from low-background IR test chambers. The instrument meets its design specifications for spectral coverage, resolution, and stability. Further tests of its performance under actual chamber calibration conditions are needed, including its sensitivity to vibrations and rf noise. While broadband spectra such as those presented here can be easily corrected for phase variation in the FTS, this correction can be more challenging for weak, narrowband spectra. Tests of the interferometric phase stability are currently being performed.

7. REFERENCES

1. Adriaan C. Carter, Raju U. Datla, and Timothy M. Jung, "Calibration of low-background temperature IR test chambers used to calibrate space sensors," *Metrologia* **46**, S213-S218 (2009).
2. Philippe Lagueux, Martin Chamberland, Frédérick Marcotte, André Villemaire, Marc Duval, Jérôme Genest, and Adriaan Carter, "Performance of a cryogenic Michelson interferometer," *Proc. of SPIE* **6692**, 669209-1 to 669209-11 (2007).
3. *Cryogenic Fourier Transform Spectrometer User's Guide*, Telops, Inc. Quebec, Canada, Revision C, p. 1 (2009).
4. Peter Griffiths and James A. DeHaseth, *Fourier Transform Infrared Spectrometry*, 2nd edition, Wiley Interscience, Chapter 1 (2007).
5. Louis Belhumeur and Andre Villemaire, *Cryo-FT acceptance test report*, Telops, Inc. Quebec, Canada, Revision E, sections 3 and 4 (2009).